

# Highly Stable Passive Wireless Sensor for Protease Activity Based on Fatty Acid-Coupled Gelatin Composite Films

Palraj Kalimuthu, Juan F. Gonzalez-Martinez, Tautgirdas Ruzgas, and Javier Sotres\*



Cite This: *Anal. Chem.* 2020, 92, 13110–13117



Read Online

ACCESS |



Metrics & More

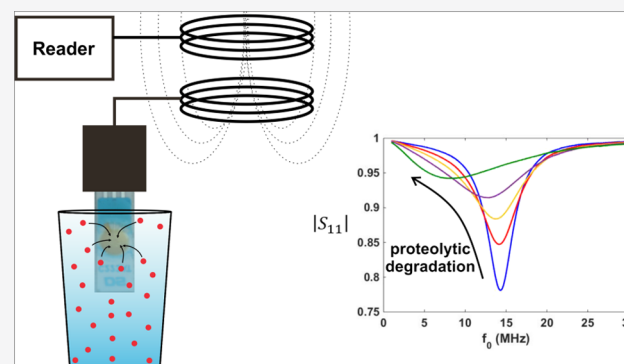


Article Recommendations



Supporting Information

**ABSTRACT:** Proteases are often used as biomarkers of many pathologies as well as of microbial contamination and infection. Therefore, extensive efforts are devoted to the development of protease sensors. Some applications would benefit from wireless monitoring of proteolytic activity at minimal cost, e.g., sensors embedded in care products like wound dressings and diapers to track wound and urinary infections. Passive (batteryless) and chipless transponders stand out among wireless sensing technologies when low cost is a requirement. Here, we developed and extensively characterized a composite material that is biodegradable but still highly stable in aqueous media, whose proteolytic degradation could be used in these wireless transponders as a transduction mechanism of proteolytic activity. This composite material consisted of a cross-linked gelatin network with incorporated caprylic acid. The digestion of the composite when exposed to proteases results in a change of its resistivity, a quantity that can be wirelessly monitored by coupling the composite to an inductor–capacitor resonator, i.e., an antenna. We experimentally proved this wireless sensor concept by monitoring the presence of a variety of proteases in aqueous media. Moreover, we also showed that detection time follows a relationship with protease concentration, which enables quantification possibilities for practical applications.



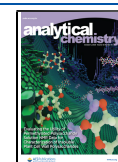
Wireless sensor technologies have an enormous potential to change the healthcare landscape.<sup>1</sup> In home environments, constant monitoring by means of wireless biosensors will allow early detection of a variety of conditions and, therefore, acting appropriately on time reducing the length and severity of required treatments. Here, the wireless aspect is of critical importance as it facilitates remote real-time measurements with minimal human intervention.<sup>2</sup> Thus, the development of wireless chemical/biological sensors is an area that has attracted significant research efforts.<sup>3–5</sup> In this work, we continue this research direction and present a novel strategy for low-cost wireless sensors for proteolytic activity.

Proteolytic activity monitoring is of high relevance in healthcare applications. Disruption of proteolytic activity is associated with many pathologies.<sup>6,7</sup> Proteolytic activity is also a biomarker for microorganisms and, subsequently, for related conditions.<sup>8</sup> Multiple methods, based on different detection principles, have been developed to quantify proteolytic activity, e.g., fluorescence-based techniques, electrochemical methods, surface spectroscopy techniques, and enzyme-linked peptide protease assays.<sup>9</sup> Any of these methods can be rendered wireless by coupling adequate circuitry (e.g., Wi-Fi, Bluetooth, etc.) to the signal-reading unit. However, in some cases, this is of little use, especially in the case of lab methods not suited for point-of-care applications. In some others, e.g., electrochemical methods, this approach still requires embedding batteries

within the sensor, which increases cost and limits implementation in many areas. One example is the incorporation of sensors in care products like wound dressings and diapers where, because of being disposable products, costs need to be kept to a minimum. For instance, incorporation of protease sensors in wound dressings would allow home monitoring of wound healing. In this regard, there is a large body of evidence that protease content (especially metalloproteinases and elastase with typical concentrations in wound fluid in the order of  $\mu\text{g/mL}$ ) reach higher values in nonhealing wounds.<sup>10,11</sup>

A different possibility is to make use of passive wireless technologies i.e., those that do not require an energy source. These can be classified according to the incorporation of an integrated circuit (chip) in the transponder/sensor. Technologies that make use of chips, like passive RFID and NFC,<sup>12–14</sup> allow the transmission of digitalized information. However, the cost of the chip still limits their implementation

Received: May 19, 2020  
Accepted: August 31, 2020  
Published: August 31, 2020



in some applications. An alternative is the use of chipless approaches.<sup>15,16</sup> These can be implemented by means of batteryless circuits/transponders that include an LC (inductor–capacitor) resonator, i.e., an antenna, that can be optionally connected to other, e.g., sensing, passive components. The reading protocol in this implementation can vary. One of the most common approaches is monitoring the frequency for which the power transmitted from a magnetically coupled network analyzer-like device also equipped with an antenna is maximized.<sup>17</sup> This (characteristic) frequency depends on the equivalent impedance of the transponder. Chemical/biosensor concepts based on this technology rely on processes where the transponder overall impedance and, therefore, the characteristic frequency, are modified in the presence of an analyte of interest.<sup>4,18–27</sup> This can be achieved in different ways. One relies on analyte-induced changes of the permeability of the surroundings of the whole transponder.<sup>4,20,21,24,28</sup> However, this sensing mechanism is limited in some cases, especially when sensing takes place in aqueous media. The presence of water in the surroundings of the antenna decreases the reading distance.<sup>29</sup> Additionally, the characteristic frequency not only depends on the transponder equivalent impedance but also on the magnetic permeability and dimensions of the different media that separate antenna and reader. Thus, the characteristic frequency would depend, e.g., on the volume of water surrounding the antenna, a parameter difficult to standardize if sampling is to be avoided. These drawbacks can be overcome with a design where the sensor section of the transponder, that is susceptible to analyte-induced impedance changes, is connected but well differentiated from the antenna section, which is kept outside the investigated aqueous medium.<sup>30</sup>

Based on this last approach, the goal of this work was to develop a sensor section that, when connected to an LC resonator/antenna, would enable wireless monitoring proteolytic activity in aqueous media. As a transduction mechanism, we focused on proteolytic degradation of biodegradable materials. This mechanism has been employed in different protease sensing approaches, often using gelatin as the biodegradable material.<sup>31–33</sup> It was also used recently for passive chipless wireless protease sensing by monitoring permeability (antenna capacitance) changes originated by the degradation of a gelatin film in the proximity of the antenna.<sup>34</sup> However, pristine gelatin films present low stability and resistivity in aqueous media. This limits their use (i) for long-term monitoring and (ii) in implementations where it would be desirable to monitor a change in resistivity rather than in permeability (which is the case for the proposed implementation). For overcoming these drawbacks, we developed a cross-linked gelatin–caprylic acid composite characterized by a high stability, surface adherence, and resistivity in aqueous media. By coupling two electrodes bridged by this composite to an antenna (LC resonator), we were able to monitor a variety of proteases and showed that this approach even enabled their quantification.

## ■ EXPERIMENTAL SECTION

**Chemicals.** Gelatin (Type A, Prod. No. G2500), glycerol (Prod. No. G5516), caprylic acid (Prod. No. O3907), aqueous solutions of glutaraldehyde (GTA) (50%, w/v) (Prod. No. G7651), proteinase from *Aspergillus melleus* (Prod. No. P4032), trypsin from porcine pancreas (Prod. No. T7409), proteinase K from *Tritirachium album* (Prod. No. P2308), and

phosphate-buffered saline (PBS) tablets (Prod. No. P4417) were procured from Sigma-Aldrich (St. Louis, MO). All solutions were prepared with ultrahigh-quality water (UHQ; resistivity, 18.2 M $\Omega$ -cm) processed in Elgastat UHQ II apparatus (Elga Ltd., High Wycombe, Bucks, England). Stock enzyme solutions (10 mg/mL in 10 mM PBS solutions) were stored at  $-70^{\circ}\text{C}$  and thawed and diluted just before use. Unless specifically stated, all chemicals used were of at least analytical grade.

**Preparation and Film Formation of Cross-Linked Gelatin–Caprylic Acid Composites.** Pristine gelatin solutions were prepared by dissolving (10% w/v) gelatin powder in UHQ water under heating ( $50^{\circ}\text{C}$ ) and continuous stirring for 30 min. Glycerol was then added until a final 1% w/v concentration and kept under heating and stirring for additional 15 min. After achieving a homogeneous gelatin–glycerol mixture, caprylic acid (CA) was added into the complex mixture until a final concentration of 64% w/v. Stirring and heating continued for 30 min until a uniform composite solution was achieved.

The resulting hot gelatin–glycerol–CA composite was used to form films both on sensor surfaces used for Quartz Crystal Microbalance with Dissipation (QCM-D) investigations and on screen-printed gold electrodes (SPGE) used for impedance and wireless investigations. For forming films on QCM-D sensor surfaces, 40  $\mu\text{L}$  of the composite were spin-coated (30 rpm, spin-coater developed in-house). The thickness of these coatings was estimated from QCM-D measurements. Coatings on SPGEs were formed by drop coating 60  $\mu\text{L}$  of the gelatin–glycerol–CA composite. In this case, thickness was estimated by differential-contrast optical microscopy (Supporting Information Section S1) (Nikon Optiphot, Japan).

After coating, the films were cooled at room temperature for 10 min and then incubated in a 0.5 wt% 5 mL glutaraldehyde (GTA) in water solution for 1 h. After this step, the films were rinsed thoroughly with UHQ water to remove any non-cross-linked GTA. Finally, the films were cured at room humidity and temperature for 12 h.

**Quartz Crystal Microbalance with Dissipation (QCM-D).** QCM-D measurements were performed with an E4 system (Q-Sense AB, Sweden) by simultaneously monitoring frequency and dissipation shifts for composite coatings formed on gold-coated AT-cut piezoelectric quartz crystals (QSX 301, Q-Sense AB, Sweden). A detailed description of the technique and its basic principles can be found elsewhere.<sup>35,36</sup>

Before every experiment, QCM-D surfaces were rinsed with Hellmanex II 2% (v/v) water solution, rinsed again extensively with UHQ water, dried under nitrogen, and plasma-cleaned for 4 min in low-pressure residual air using a glow discharge unit (PDC-32 G, Harrick Scientific Corp.).

Noncoated QCM-D sensors were initially characterized in PBS solution. Then, they were removed from the instrument and subsequently spin-coated with the gelatin-based composite (see above). Then, the coated sensors were again characterized by QCM-D in PBS for 5 h and, subsequently, in the presence of protease solutions.

**Vector Network Analyzer (VNA).** A commercial DG8-SAQ VNA (SDR-Kits, Melksham, U.K.) was used both to characterize the impedance of cross-linked gelatin–CA composites and as a reader for the proposed wireless sensor concept. For this, the SPGEs (C223AT, Metrohm DropSens, Spain) were coated with the composite as previously indicated. The working and counter electrodes of the SPGEs were

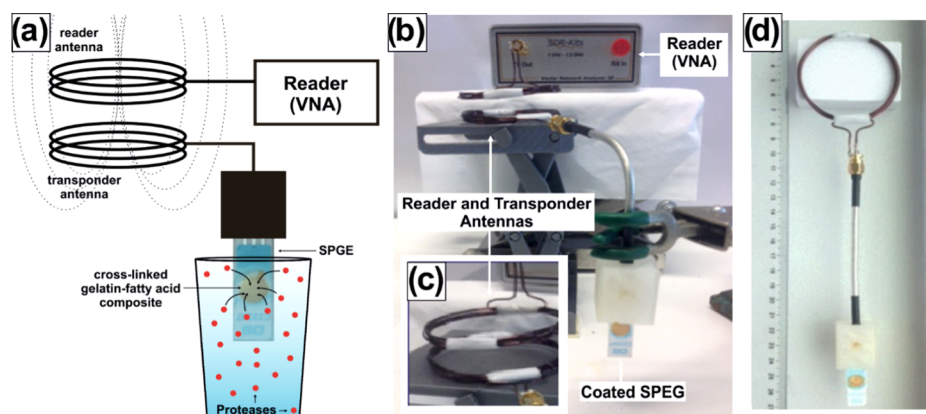


**Figure 1.** (a) Illustration and (b) photograph of the setup used for wireless protease detection. (c) Close view of the reader and transponder antennas. (d) Prototype of the proposed wireless protease sensor.

connected to a 50  $\Omega$  coaxial cable (matching the characteristic impedance of the VNA) by means of a homemade three-dimensional (3D) printed holder (Figure 1, the reference electrode was unattended). For direct impedance measurement, the opposite end of the coaxial cable was connected to the transmitter port (TX) of the VNA. For wireless measurements, a homemade copper circular RF antenna (diameter 5.5 cm, five loops) was soldered to the end of the coaxial cable (Figure 1). A similar RF antenna was connected to the TX port of the VNA (Figure 1) so that it functioned as a wireless reader. For all reported experiments, reader and sensor antenna were kept at a distance of 1.2 cm.

Both direct and wireless VNA-based measurements were performed by first exposing the composite-coated SPGEs to bare PBS for at least 24 h to ensure stability.

Then, the coated SPGEs were exposed to protease solutions and the magnitude of the reflection scattering parameter,  $|S_{11}| = \sqrt{1 - \frac{P_T}{P_{\max}}}$  (where  $P_T$  is the transmitted power and  $P_{\max}$  is the maximum achievable transmitted power) was monitored continuously in the 3–30 MHz range at a sweep rate of 135 kHz/s. For experiments where the proteolytic degradation took long times, the protease solution was replaced every 48 h to counteract the decrease of enzyme activity.

## RESULTS AND DISCUSSION

**Sensor Concept.** In this work, we propose a concept for passive radio frequency (RF) wireless sensing of proteases based on a transponder design with well-differentiated antenna and sensor sections, only the latter being exposed to the investigated aqueous media. The equivalent circuit for this concept is shown in Figure 2.

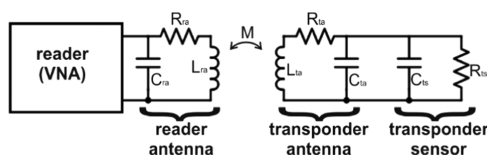


**Figure 2.** Equivalent circuit for the reader and proposed transponder/sensor concept. The reader antenna is magnetically coupled ( $M$ ) to the transponder antenna. Both antennas are modeled as series  $RLC$  circuits. In the transponder, the antenna section is connected to a sensor section (in our case, a biodegradable polymeric material) modeled by a capacitor and a resistor connected in parallel.

In this concept, the power transmitted from the reader antenna to the transponder is maximized, i.e., the power reflected is minimized, for a (characteristic) frequency for which the imaginary part of the equivalent impedance (eq 1) is zero<sup>37</sup>

$$Z_{\text{eq}} = Z_{\text{reader\_antenna}} + \frac{\omega^2 M^2}{Z_{\text{transponder}}} \quad (1)$$

where  $M$  is the mutual inductance between reader and transponder antennas. The impedance for the reader antenna can be expressed as

$$Z_{\text{reader\_antenna}} = \left[ \frac{1}{j\omega C_{ra}} + \frac{1}{R_{ra} + j\omega L_{ra}} \right]^{-1} \quad (2)$$

whereas the impedance for the transponder would be

$$\begin{aligned} Z_{\text{transponder}} &= j\omega L_{ta} + R_{ta} + \frac{R_{ts}}{1 + j\omega(C_{ta} + C_{ts})R_{ts}} = \\ &= R_{ta} + \frac{R_{ts}}{1 + [\omega(C_{ta} + C_{ts})R_{ts}]^2} \\ &\quad + j \left\{ \omega L_{ta} - \frac{\omega(C_{ta} + C_{ts})R_{ts}^2}{1 + [\omega(C_{ta} + C_{ts})R_{ts}]^2} \right\} \end{aligned} \quad (3)$$

where  $L_{ra}$ ,  $R_{ra}$ , and  $C_{ra}$  correspond to the inductance and parasitic resistance and capacitance of the reader antenna,  $L_{ta}$ ,  $R_{ta}$ , and  $C_{ta}$  correspond to those of the transponder antenna, and  $C_{ts}$  and  $R_{ts}$  correspond to the capacitance and resistance of the transponder sensor section. It is not straightforward to identify how the characteristic frequency, i.e., for which the imaginary part of  $Z_{\text{eq}}$  becomes zero, depends on  $R_{ts}$  and  $C_{ts}$  because of the complexity of the corresponding analytical expression. However, it is possible to arrive at a simpler expression if one can neglect the contribution from the reader antenna, i.e., if the reader and transponder antennas resonate at significantly different frequencies (as it was the case for our setup, Supporting Information Section S2). In this situation, it is reasonable to assume that the power reflected will be minimized for a frequency close to that for which the imaginary part of the equivalent impedance of the transponder is zero. From eq 3 follows that the condition  $\text{Im}\{Z_{\text{transponder}}\} = 0$  is fulfilled for a characteristic frequency  $\omega_0$  such that (eq 4)

$$\omega_0 = \sqrt{\frac{1}{L_{ta}(C_{ta} + C_{ts})} - \frac{1}{[(C_{ta} + C_{ts})R_{ts}]^2}} \quad (4)$$

From eq 4, it follows that a decrease in the resistance of the sensor section of the transponder,  $R_{ts}$ , would lower the frequency for which the reflected power is minimized. In the proposed sensor concept, we make use of this dependence.

**Development of a Gelatin-Based Material Suitable for Wireless Monitoring of Proteolytic Activity.** Following previous works,<sup>31,32,34,38,39</sup> we focused on gelatin as the main component of the biodegradable material to be incorporated in our transponder design. However, the use of pristine gelatin films on impedance-based sensors has inherent drawbacks. The reason is that the impedance of pristine gelatin films is similar to that of physiological aqueous media and only starts to differ for very low ionic strengths (<2 mM).<sup>32,39</sup> This limited the use of pristine gelatin in our transponders. Specifically, the characteristic frequency measured in physiological media for transponders with sensor sections consisting of pristine gelatin films did not significantly differ from that measured for transponders with sensor sections consisting of noncoated electrodes (Supporting Information Section S3). Thus, further improvements of the degradable material to be used were required.

We first incorporated glycerol as a plasticizer to increase film wettability and adhesiveness.<sup>32,39</sup> Glycerol also enhances water permeability and, therefore, decreases stability due to the presence of hydrophilic OH groups.<sup>40</sup> For this reason, we kept the amount of glycerol down to a minimum (1% w/v).

To further increase resistivity, gelatin was cross-linked, specifically with glutaraldehyde (GTA) because of its low cost and effectiveness.<sup>33,41</sup> Bigi and co-workers<sup>41</sup> investigated the efficiency of GTA in cross-linking gelatin and reported that 98% cross-linking was achieved when exposing gelatin to 0.5 wt% GTA in water solution. We used a similar concentration. This choice was supported by the fact that (i) for lower GTA concentrations, fast film detachment and solubilization were observed, and (ii) for this value, the wireless sensors exhibited a stable characteristic frequency that could be clearly differentiated from that of transponders with noncoated sensor sections (Supporting Information Section S3).

To further reduce the water permeability of gelatin films, we incorporated fatty acids.<sup>42</sup> As fatty acids with chain lengths exceeding 12 carbon atoms do not homogeneously mix up with gelatin,<sup>42</sup> we chose caprylic acid, CA ( $C_8H_{16}O_2$ ). We performed a systematic study on the optimal CA concentration to be used and found that 64% w/v was optimal not only for achieving a well-differentiated characteristic frequency upon coating the SPEG with the composite but also for increasing the transmitted power between reader and sensor and, therefore, expanding the reading range (Supporting Information Section S3).

The successful incorporation of CA and GTA into the pristine gelatin films was confirmed by means of Fourier transform infrared (FTIR) spectroscopy (Supporting Information Section S4). Moreover, the developed composite exhibited appropriate characteristics for its use in wireless proteolytic detection, as shown and discussed below.

**Proteolytic Degradability of GTA Cross-Linked Gelatin–CA Composites.** The performance of the proposed sensor relies on the susceptibility to proteolytic degradation of the developed gelatin-based composites. This was investigated by QCM-D monitoring the composites exposed to a model

protease, proteinase from *A. melleus* (Figure 3). The protease choice was based on that the filamentous microfungi *Aspergillus*

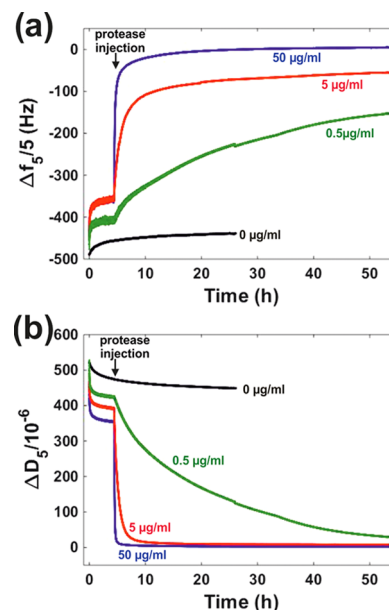


**Figure 3.** (a) Frequency and (b) dissipation shifts for the fifth overtone corresponding to representative experiments where QCM-D gold surface modified with cross-linked gelatin–CA composites were initially exposed to PBS for 5 h, followed by exposure to different concentrations of proteinase from *A. melleus* (0.5, 5, and 50  $\mu\text{g/mL}$ ) in PBS. Both plots also include a negative control where the composite was exposed to bare PBS for 26 h.

are known to cause a broad spectrum of systemic diseases<sup>43</sup> and on that their proteases are used for diverse biotechnological applications.<sup>44</sup>

Figure 3 shows frequency and dissipation shifts for the fifth overtone (similar behavior was observed for other overtones) of gold QCM-D surfaces coated with cross-linked gelatin–CA composites. In the figure, zero frequency and dissipation values correspond to those measured for clean noncoated surfaces. Values for  $t > 0$  correspond to those measured for the coated sensor immediately after exposure to PBS. Coating resulted in negative frequency and positive dissipation shifts, indicating the presence of a highly viscoelastic coating. It is possible to estimate the adsorbed mass by means of the Sauerbrey equation<sup>45</sup>

$$\frac{\Delta f_n}{n} = -\frac{2\Gamma f_0^2}{z_q} \quad (5)$$

where  $n$  is the overtone number,  $\Delta f_n$  is the frequency shift of the  $n$ th overtone,  $\Gamma$  is the adsorbed amount,  $f_0$  is the quartz fundamental frequency, and  $z_q$  is the acoustic or mechanical impedance. Even though the Sauerbrey equation underestimates the mass of a highly viscous layer as those investigated here, it still provides a reasonable estimation.<sup>31</sup>

Assuming from Figure 3 an average  $\frac{\Delta f_n}{n}$  value of  $-400$  Hz for the coatings, eq 5 yields a  $\Gamma$  of  $\sim 7 \times 10^{-6}$  g/cm<sup>2</sup>. Assuming that the density of the films would be similar to that of water (i.e., 1 g/cm<sup>3</sup>), the thickness of the coatings formed on QCM-D surfaces would be  $\sim 70$  nm. Exposure of the coatings for  $\sim 1$  h to the highest investigated protease concentration (50  $\mu\text{g/}$

mL) resulted in their effective disintegration as indicated by the fact that both frequency and dissipation shifts decreased to almost zero values. Exposure of the coatings to lower protease concentrations (5 and 0.5  $\mu\text{g}/\text{mL}$ ) also led to degradation at, however, longer times. These results proved the proteolytic degradability of the developed cross-linked gelatin–CA composites and even the possibility to use this degradability as a quantitative transducer mechanism for proteolytic activity.

**Impedance of Cross-Linked Gelatin–CA Composites during Their Proteolytic Degradation.** The proposed wireless protease sensor concept is based on that proteolytic degradation of the cross-linked gelatin–CA composites, i.e., the sensor section of the transponders, leads to a shift in the overall impedance of the transponder and, therefore, of its resonance frequency. This requires that the impedance in the RF spectrum of the sensor section, i.e., the composite-bridged electrodes, also changes in the presence of proteases. We verified this behavior by means of VNA measurements, as indicated in the [Experimental Section](#).

Here, we used thicker composite films (Supporting Information [Section S1](#)) than in QCM-D experiments. The rationale behind this was achieving long-time stability of the composite films in aqueous solutions ( $\sim 10^3$  h, Supporting Information [Section S5](#)). [Figure 4](#) shows a representative measurement of the real ([Figure 4a](#)) and imaginary ([Figure 4b](#)) components of the impedance of the composite-bridged electrodes from the moment they were exposed to a 0.5 mg/mL solution of proteinase from *A. melleus*. It can be seen that after ca. 27 h both components reached a stable value. We hypothesized that the system could be modeled as a capacitor,  $C$ , and a resistor,  $R$ , combined in parallel. Subsequently, we used [eq 6](#) to fit both the real and imaginary components of the composite-bridged electrodes impedance during its degradation.

$$\begin{aligned} Z_{\text{equivalent}} &= \frac{R}{1 + j2\pi fCR} \\ &= \frac{R}{1 + (2\pi fCR)^2} - j \frac{2\pi fCR^2}{1 + (2\pi fCR)^2} \end{aligned} \quad (6)$$

As shown in Supporting Material [Section S6](#), [eq 6](#) provided a reasonable fit for the experimental data. This allowed quantifying the capacitance ([Figure 4c](#)) and resistance ([Figure 4d](#)) of the setup during the proteolytic degradation of the composite coatings. It can be seen that the change in capacitance can be neglected (values stayed within a  $\sim 3$  pF window during the experiment). However, resistance decreased continuously during exposure of the composite to proteases. When the resistance reached a stable value, the composite was completely degraded as confirmed by visual inspection (Supporting Information [Section S1](#)). According to [eq 4](#), when incorporated in standard  $LC$  transponders with resonance frequency in the investigated range, degradation proteolytic digestion of cross-linked gelatin–CA composites will result in a decrease of their characteristic frequency, allowing this process to be wirelessly monitored.

**Wireless Protease Sensing in Aqueous Media.** The degradation of the developed cross-linked gelatin–CA composite films (coupled to an RF antenna, [Figure 1d](#)) was wirelessly monitored by means of the magnitude of the forward scattering parameter,  $|S_{11}|$ , registered with a VNA equipped with another RF antenna ([Figure 5](#)).  $|S_{11}|$  spectra from a representative experiment, where the composite-bridged

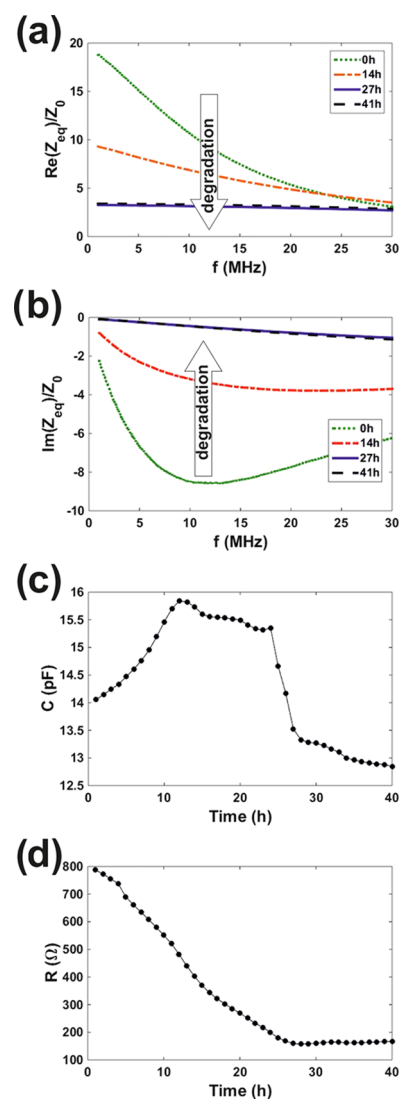


**Figure 4.** (a) Real and (b) imaginary components of the impedance of a cross-linked gelatin–CA composite-coated SPGE exposed to a 0.5 mg/mL solution of proteinase from *A. melleus* in PBS. (c) Capacitance and (d) resistance values obtained by fitting experimental impedance data from (a) and (b) to [eq 6](#).

electrodes, i.e., the sensor section of the transponder, were exposed to a 5 mg/mL solution of proteinase from *A. melleus* in PBS, are shown in [Figure 5a](#). The time evolution of the transponder characteristic frequency,  $f_0$  (that for which  $|S_{11}|$  reached a minimum value), for four different experiments where the wireless sensors were exposed to different protease concentrations (5, 0.5, 0.05, and 0.005 mg/mL) in PBS are shown in [Figure 5b](#). These figures evidence that  $f_0$  started to decrease soon after exposure to proteases until, eventually, a stable value was reached. The  $f_0$  decrease rate was significantly faster than that observed in control experiments where the composite-coated electrodes were exposed to protease-free PBS. In these control experiments,  $f_0$  decreased less than 0.5 MHz during the initial 800 h of buffer exposure (Supporting Information [Section S5](#)).

As seen in [Figure 5b](#), the rate at which  $f_0$  decreased with exposure time increased significantly after an initial 0.8 MHz shift. Subsequently, we used this  $f_0$  shift, i.e., 0.8 MHz, as a protease detection criterion. According to this criterion,

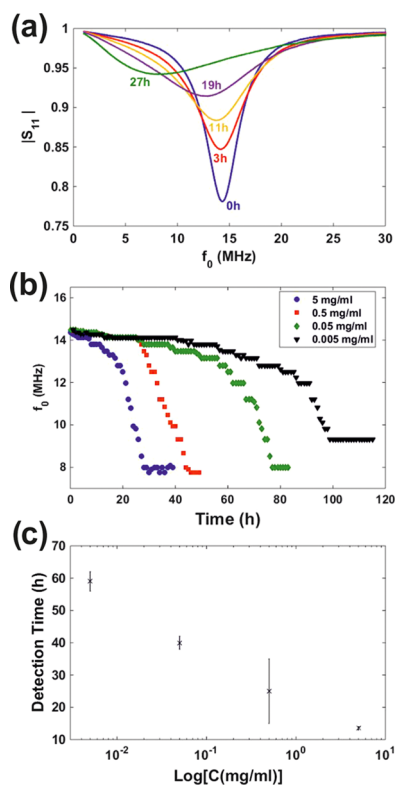


**Figure 5.** (a)  $|S_{11}|$  time evolution for a representative experiment where one of the developed protease sensors was exposed to 5 mg/mL of proteinase from *A. melleus*. (b) Evolution of the characteristic frequency over time measured for different sensors exposed to different concentrations of proteinase from *A. melleus*. (c) Protease detection time, defined at that for which the characteristic frequency of sensors exposed to protease solutions shifted by 0.8 MHz, for different concentrations of proteinase from *A. melleus* in PBS.

proteinase from *A. melleus* was detected at  $13.5 \pm 0.5$  h for a bulk concentration of 5 mg/mL, at  $25 \pm 10$  h for a bulk concentration of 0.5 mg/mL, at  $40 \pm 2$  h for a bulk concentration of 0.05 mg/mL, and at  $59 \pm 3$  h for a bulk concentration of 0.005 mg/mL. Figure 5c shows that protease detection times exhibited an exponential-like dependence with bulk protease concentration. While more data points would be needed to properly define a calibration standard, our results sufficiently show that the proposed sensor concept not only allows monitoring the presence of proteases but also shows possibilities for calibration and, therefore, for protease quantification.

Our results were obtained under physiological ionic strength conditions. As changes in  $f_0$  originate from changes in the resistivity between the coated electrodes, it is expected that ionic strength will influence both the final  $f_0$  value and its change rate during the degradation process (the initial value is almost independent of the surrounding medium, as shown in Supporting Information Section S7). Subsequently, we aim to investigate the role of ionic strength in a future work.

In wireless monitoring based on LC resonance,  $f_0$  shifts can also be originated by changes in the dielectric properties of the media between reader and transponder, as well as by changes in the distance/orientation between both. The first aspect does not play a role in the employed setup. Separating antenna and sensor sections in the transponder allowed a configuration where the media, i.e., air, between the transponder antenna and

the reader does not vary. Regarding the second aspect, changes in the reader–transponder distance and relative orientation had mainly an effect in the  $|S_{11}|$  magnitude but not in  $f_0$  (Supporting Information Section S8). Thus, the monitored  $f_0$  shifts could be unequivocally ascribed to the onset of proteolytic degradation in the investigated liquid.

Finally, we also confirmed that the proposed concept could be used to monitor the presence of other proteases of different origin, as shown in Supporting Information Section S9, for trypsin and proteinase K from *Tritirachium album*.

Nonspecificity is a characteristic feature of most heterogeneous protease assays that make use of natural substrates like gelatin.<sup>9,46</sup> In this regard, the use of synthetic peptides with predetermined amino acid sequences that match the recognition sequence of the protease of interest stands out as a promising approach.<sup>47,48</sup> We foresee that the proposed wireless proteases sensor concept could be implemented with composite materials that incorporate such peptides, therefore providing selectivity for specific proteases.

## CONCLUSIONS

We present a biodegradable composite material characterized by high stability, surface adherence, and resistivity in aqueous media, and prove its potential for incorporation in passive wireless transponders for monitoring proteolytic activity. The major addressed challenge was developing a biodegradable material characterized by (i) a resistivity significantly higher than that of aqueous media, (ii) highly stable in these media to enable long-term monitoring, but (iii) that could still be degradable by proteases. For this, we developed, and extensively characterized, a cross-linked gelatin–caprylic acid composite that fulfills these characteristics. For proving the possibility of using the degradation of this composite as a transduction mechanism for passive wireless monitoring of proteases, we propose a concept where the wireless transponder consists of well-differentiated antenna (LC resonator) and sensor sections. In turn, the sensor section consists of electrodes bridged by the biodegradable composite. We showed that proteolytic digestion of the composite leads to a change in its resistivity, which eventually decreases to that of the aqueous environment. This results in a change of the overall impedance of the transponder and, subsequently, in a decrease of the (characteristic) frequency for maximum reader–transponder transmitted power, i.e., the quantity used for wirelessly monitoring in passive wireless communication. We experimentally proved the validity of this sensor concept by successfully monitoring the presence of a variety of proteases in aqueous media. Moreover, we also showed that detection time follows a relationship with protease bulk concentration, which opens quantification possibilities. Finally, while it is clear that the developed cross-linked gelatin–caprylic acid composite has substantial potential for applications that would benefit from wireless monitoring of proteolytic activity, it is worth to mention that it could as well be incorporated in any other type of electrical chemical sensor strategy regardless of the reading mechanism.

## ASSOCIATED CONTENT

### Supporting Information

The Supporting Information is available free of charge at <https://pubs.acs.org/doi/10.1021/acs.analchem.0c02153>.

Optical characterization of SPGEs, antenna's impedances, composite composition optimization; FTIR spectra of composite and composite stability on aqueous medium; composite impedance during degradation; role of ambient medium and reader–transponder distance/orientation in the characteristic frequency; and wireless monitoring of proteinase K and trypsin (PDF)

## AUTHOR INFORMATION

### Corresponding Author

Javier Sotres – Department of Biomedical Science, Faculty of Health and Society and Biofilms-Research Center for Biointerfaces, Malmö University, 20506 Malmö, Sweden;  
orcid.org/0000-0001-6937-3057; Email: javier.sotres@mau.se

### Authors

Palraj Kalimuthu – Department of Biomedical Science, Faculty of Health and Society and Biofilms-Research Center for Biointerfaces, Malmö University, 20506 Malmö, Sweden

Juan F. Gonzalez-Martinez – Department of Biomedical Science, Faculty of Health and Society and Biofilms-Research Center for Biointerfaces, Malmö University, 20506 Malmö, Sweden

Tautgirdas Ruzgas – Department of Biomedical Science, Faculty of Health and Society and Biofilms-Research Center for Biointerfaces, Malmö University, 20506 Malmö, Sweden

Complete contact information is available at:

<https://pubs.acs.org/10.1021/acs.analchem.0c02153>

### Author Contributions

The manuscript was written through contributions of all authors. All authors have given approval to the final version of the manuscript.

### Notes

The authors declare no competing financial interest.

## ACKNOWLEDGMENTS

The Knowledge Foundation (grant nos. 20150207 and 20190010), the Swedish Research Council (grant no. 2018-04320), the Mats Paulsson's foundation for research, innovation and development of society, Malmö University, and the Gustav Th. Ohlsson Foundation are gratefully acknowledged for financial support.

## REFERENCES

- (1) Alemdar, H.; Ersoy, C. *Comput. Networks* **2010**, *54*, 2688–2710.
- (2) Ghafar-Zadeh, E. *Sensors* **2015**, *15*, 3236–3261.
- (3) Kassal, P.; Steinberg, M. D.; Steinberg, I. M. *Sens. Actuators, B* **2018**, *266*, 228–245.
- (4) Potyrailo, R. A.; Nagraj, N.; Tang, Z.; Mondello, F. J.; Surman, C.; Morris, W. J. *Agric. Food Chem.* **2012**, *60*, 8535–8543.
- (5) Steinberg, M. D.; Kassal, P.; Steinberg, I. M. *Electroanalysis* **2016**, *28*, 1149–1169.
- (6) Wilkinson, R. D. A.; Williams, R.; Scott, C. J.; Burden, R. E. *Biol. Chem.* **2015**, *396*, 867.
- (7) Yuan, J.; Yankner, B. A. *Nature* **2000**, *407*, 802–809.
- (8) McKerrow, J. H.; Caffrey, C.; Kelly, B.; Loke, Pn.; Sajid, M. *Annu. Rev. Pathol.: Mech. Dis.* **2006**, *1*, 497–536.
- (9) Ong, I. L. H.; Yang, K.-L. *Analyst* **2017**, *142*, 1867–1881.
- (10) Ladwig, G. P.; Robson, M. C.; Liu, R.; Kuhn, M. A.; Muir, D. F.; Schultz, G. S. *Wound Repair Regen.* **2002**, *10*, 26–37.

- (11) McCarty, S. M.; Percival, S. L. *Adv. Wound Care* **2013**, *2*, 438–447.
- (12) Abrar, M. A.; Dong, Y.; Lee, P. K.; Kim, W. S. *Sci. Rep.* **2016**, *6*, No. 30565.
- (13) Kassal, P.; Kim, J.; Kumar, R.; de Araujo, W. R.; Steinberg, I. M.; Steinberg, M. D.; Wang, J. *Electrochem. Commun.* **2015**, *S6*, 6–10.
- (14) Martínez-Olmos, A.; Fernández-Salmerón, J.; Lopez-Ruiz, N.; Rivadeneyra Torres, A.; Capitan-Vallvey, L. F.; Palma, A. J. *Anal. Chem.* **2013**, *85*, 11098–11105.
- (15) Finkenzeller, K. *RFID Handbook*; John Wiley & Sons, Ltd: Wiltshire, UK, 2010.
- (16) Karmakar, N. C.; Amin, E. M.; Saha, J. K. *Chipless RFID Sensors*; John Wiley & Sons: Hoboken, New Jersey, 2016.
- (17) Lee, H.-J.; Yook, J.-G. *Biosens. Bioelectron.* **2014**, *61*, 448–459.
- (18) Chien, J. H.; Chen, P. H.; Kuo, L. S.; Lin, C. S.; Wang, H. *Appl. Phys. Lett.* **2007**, *91*, No. 143901.
- (19) Kim, N. Y.; Dhakal, R.; Adhikari, K. K.; Kim, E. S.; Wang, C. *Biosens. Bioelectron.* **2015**, *67*, 687–693.
- (20) Kim, N.-Y.; Adhikari, K. K.; Dhakal, R.; Chuluunbaatar, Z.; Wang, C.; Kim, E.-S. *Sci. Rep.* **2015**, *5*, No. 7807.
- (21) Lee, H.-J.; Lee, J.-H.; Jung, H.-I. *Appl. Phys. Lett.* **2011**, *99*, No. 163703.
- (22) Mannoor, M. S.; Tao, H.; Clayton, J. D.; Sengupta, A.; Kaplan, D. L.; Naik, R. R.; Verma, N.; Omenetto, F. G.; McAlpine, M. C. *Nat. Commun.* **2012**, *3*, No. 763.
- (23) Park, H.; Seo Yoon, H.; Patil, U.; Anoop, R.; Lee, J.; Lim, J.; Lee, W.; Chan Jun, S. *Biosens. Bioelectron.* **2014**, *54*, 141–145.
- (24) Potyrailo, R. A.; Morris, W. G. *Anal. Chem.* **2007**, *79*, 45–51.
- (25) Ruzgas, T.; Larpant, N.; Shafaat, A.; Sotres, J. *ChemElectroChem* **2019**, *6*, 5167–5171.
- (26) Tanguy, N. R.; Fiddes, L. K.; Yan, N. *ACS Appl. Mater. Interfaces* **2015**, *7*, 11939–11947.
- (27) Yuan, M.; Alocilja, E. C.; Chakrabarty, S. *IEEE Sens. J.* **2014**, *14*, 941–942.
- (28) Reuel, N. F.; McAuliffe, J. C.; Becht, G. A.; Mehdizadeh, M.; Munos, J. W.; Wang, R.; Delaney, W. J. *ACS Sens.* **2016**, *1*, 348–353.
- (29) Jiang, S.; Georgakopoulos, S. J. *Electromagn. Anal. Appl.* **2011**, *3*, 261–266.
- (30) Larpant, N.; Pham, A. D.; Shafaat, A.; Gonzalez, J. F.; Sotres, J.; Sjöholm, J.; Laiwattanapaisal, W.; Faridbod, F.; Ganjali, M. R.; Arnebrant, T.; Ruzgas, T. *Sci. Rep.* **2019**, *9*, No. 12948.
- (31) Bahmanzadeh, S.; Ruzgas, T.; Sotres, J. J. *Colloid Interface Sci.* **2018**, *526*, 244–252.
- (32) Banis, G.; Beardslee, L. A.; Ghodssi, R. *Appl. Sci.* **2018**, *8*, 208.
- (33) Schyrr, B.; Boder-Pasche, S.; Ischer, R.; Smajda, R.; Voirin, G. *Sens. Biosens. Res.* **2015**, *3*, 65–73.
- (34) Charkhabi, S.; Beierle, A. M.; McDaniel, M. D.; Reuel, N. F. *ACS Sens.* **2018**, *3*, 1489–1498.
- (35) Rodahl, M.; Höök, F.; Fredriksson, C.; A. Keller, C.; Krozer, A.; Brzezinski, P.; Voinova, M.; Kasemo, B. *Faraday Discuss.* **1997**, *107*, 229–246.
- (36) Rodahl, M.; Höök, F.; Krozer, A.; Brzezinski, P.; Kasemo, B. *Rev. Sci. Instrum.* **1995**, *66*, 3924–3930.
- (37) Alexander, C. K.; Sadiku, M. N. O. *Fundamentals of Electric Circuits*, 6th ed.; McGraw-Hill: New York, 2017.
- (38) Ionescu, R. E.; Fillit, C.; Jaffrezic-Renault, N.; Cosnier, S. *Biosens. Bioelectron.* **2008**, *24*, 489–492.
- (39) Saum, A. G. E.; Cumming, R. H.; Rowell, F. J. *Biosens. Bioelectron.* **1998**, *13*, 511–518.
- (40) Nilsuwan, K.; Benjakul, S.; Prodpran, T. *J. Food Sci. Technol.* **2016**, *53*, 2715–2724.
- (41) Bigi, A.; Cojazzi, G.; Panzavolta, S.; Rubini, K.; Roveri, N. *Biomaterials* **2001**, *22*, 763–768.
- (42) Fakhouri, F. M.; Fontes, L. C. B.; Innocentini-Mei, L. H.; Collares-Queiroz, F. P. *Starch-Stärke* **2009**, *61*, 528–536.
- (43) Zotti, M.; Agnoletti, A. F.; Vizzini, A.; Cozzani, E.; Parodi, A. *Exp. Dermatol.* **2015**, *24*, 966–968.
- (44) Miyazawa, T.; Hiramatsu, M.; Murashima, T.; Yamada, T. *Biocatal. Biotransform.* **2003**, *21*, 93–100.

- (45) Sauerbrey, G. *Z. Phys.* **1959**, *155*, 206–222.
- (46) Kaman, W. E.; Hays, J. P.; Endtz, H. P.; Bikker, F. J. *Eur. J. Clin. Microbiol. Infect. Dis.* **2014**, *33*, 1081–1087.
- (47) Chen, H.; Mei, Q.; Hou, Y.; Zhu, X.; Koh, K.; Li, X.; Li, G. *Analyst* **2013**, *138*, 5757–5761.
- (48) Esseghaier, C.; Ng, A.; Zourob, M. *Biosens. Bioelectron.* **2013**, *41*, 335–341.